

Robust Metal-Ceramic Coaxial Cable Sensors for Distributed Temperature Monitoring in Fossil Energy Power Systems

UCR Project Number: *DE-FE-0022993*

DOE Project Manager: *Jessica Mullen*

Project Duration: *07/01/2014 – 06/30/2017*

Principal Investigators: *Junhang Dong (PI) and Hai Xiao (CoPI)*

Student Participants: *Adam Trontz and Shixuan Zeng (U. Cincinnati)*

Baokai Chen and Wenge Zhu (Clemson U.)

Chemical Engineering/CEAS, University of Cincinnati

Dept. Electrical Engineering and Computer Science, Clemson University

Crosscutting Research Project Review Meeting, March 20-23, 2017, Pittsburgh, PA

National Energy Research Program/NETL, U.S. Department of Energy



Outline

- Introduction
- Project objective, tasks and status
 - Concept of proposed MCCC-FPI
 - Technical Challenges
 - Research Objective
 - Tasks/milestones/timeline
- Research accomplishments
 - Materials identification and development
 - Single point MCCC-FPI sensor
 - Multi-point (2~3) MCCC-FPI sensor
 - Long cable (2m) multi-point (10pts) sensor
 - MCCC-FPI for MW frequency ϵ_r measurement
- Conclusion

Introduction

- **High temperature measurements in advanced fossil fuel power plants:**

- Needs for real-time distributed temperature measurement for
 - Process control
 - Performance enhancement
 - Safety assurance (equipment, environment, and human)
- Temperature sensors must
 - survive and function in corrosive gases ($T \geq 1000^{\circ}\text{C}$ and $P > 1000$ Psi)
 - possess mechanical strength and small size for ease of installation with reliability,
 - have high sensitivity,
 - provide distributed sensing on single string covering large distance/area
 - be of low cost.

- **Current technologies**

- 1) Thermocouples, Pyrometer ... (point measurement;)
- 2) Fiber optic sensors ($< 800^{\circ}\text{C}$...)

Research Objective

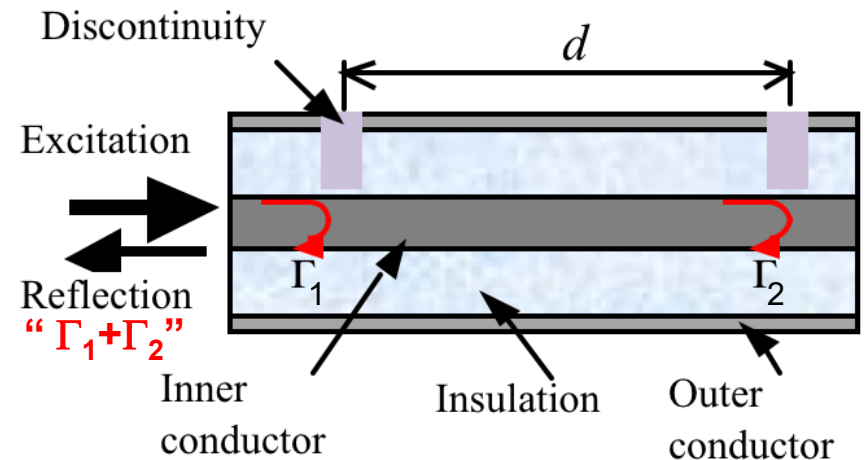
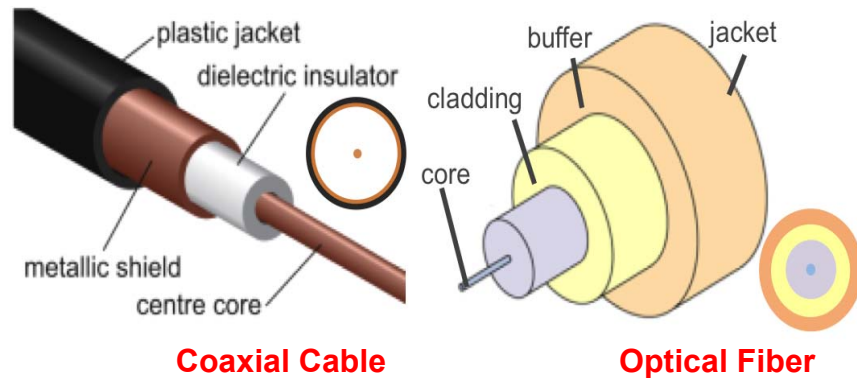
- **Project Goal:**

- To develop materials for a new type of low cost, robust, (minimum packaging/protection) metal-ceramic coaxial cable (MCCC) Fabry-Pérot interferometer (FPI) sensor and demonstrate its capability of cascading a series of FPIs in a single MCCC for real-time distributed monitoring of temperature up to 1000°C.

- **Technical Objectives:**

- 1) to identify and develop sensor materials with desired electrical and dielectric properties as well as thermochemical and structural stability,
- 2) to develop the instrumentation for signal processing and algorithm for operating the sensor and distributed sensing systems, and
- 3) to fabricate demonstrate the MCCC-FPI sensor for real-time distributed temperature measurement and evaluate its performance in terms of sensitivity, spatial resolution, stability, and response speed that are important to practical applications.

Sensor Concept: Coaxial Cable Fabry-Pérot Interferometer (CC-FPI)



• CC-FPI sensor operation principle

- **Device:** RF interferometer (analog to fiber optic interferometer)
- **Signal:** interference of reflections from reflectors (ε disturbance)
- **Operating mechanism:** Shift of interferogram by variation of " $d \times \varepsilon_r^{0.5}$ "

CC-FPI Temperature Sensing Mechanism

- Two reflections (U_1 and U_2)

$$U_1 = \Gamma(f)e^{-\alpha z} \cos(2\pi ft) \quad \text{and} \quad U_2 = \Gamma(f)e^{-\alpha z} \cos[2\pi f(t + \tau)]$$

$$\text{where} \quad \tau = 2d\sqrt{\epsilon_r} / c \quad t = 2d_0\sqrt{\epsilon_r} / c$$

- Interference (U) – summation of U_1 and U_2

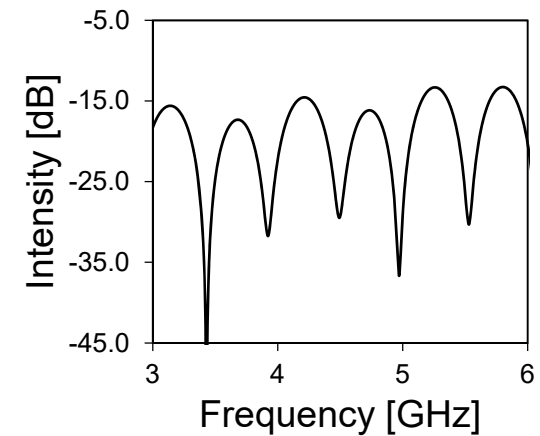
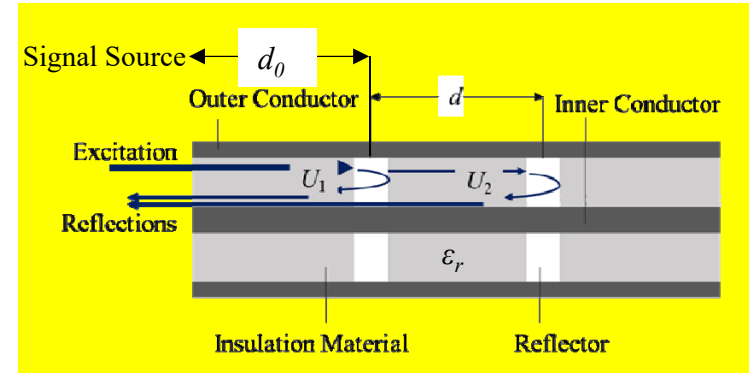
$$U = 2 \cdot \Gamma(f)e^{-\alpha z} \cos\left(\pi f \frac{2d\sqrt{\epsilon_r}}{c}\right) \cos\left[\pi f \left(\frac{4d_0\sqrt{\epsilon_r}}{c} + \frac{2d\sqrt{\epsilon_r}}{c}\right)\right]$$

- CC-FPI " d " and " ϵ_r " are temperature dependent

$$d_T = d_0 + d_0 \times b_T(T - T_0) \quad \epsilon_{r,T} = \sum_{i=0}^n (a_i \times T^i)$$

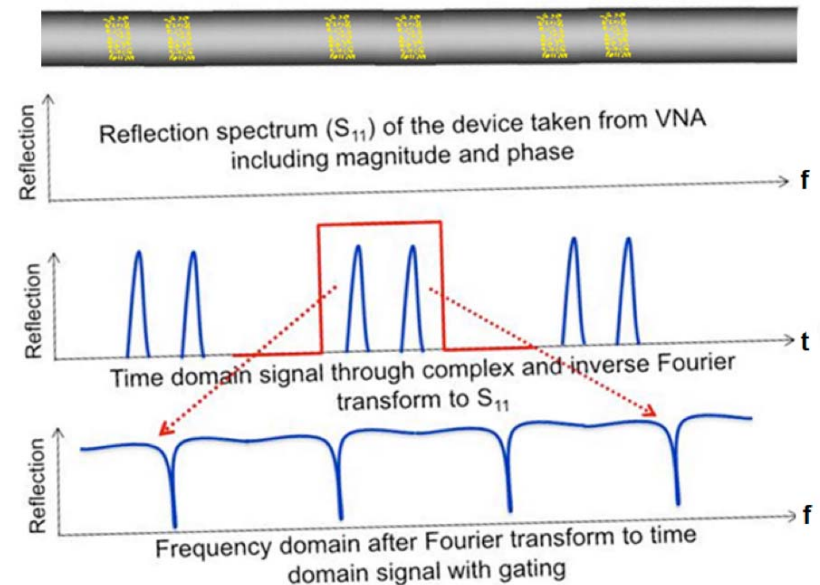
- $U(T)$ is thus a function of temperature - *real-time temperature measurement by monitoring the interferometric spectrum shift, $U(T)$*

$$U(T) = K_1 \cos(K_2 \cdot \tau(T)) \cdot \cos[K_2(t + \tau(T))] \quad \tau(T) = 2d_T \cdot \epsilon_{r,T}^{0.5} / c$$



Concept: Multiple CC-FPI Sensors for Distributed Temperature Measurement

- Distributed CC-FPI sensor – multiple FPI along a single ceramic coaxial cable
- The reflectors of weak reflections and low insertion loss enable long distance coverage (2nd reflections are negligible)
- Position by extracting and analyzing the spectrum of a specific discrete FPI - *achieved by a novel joint time-frequency domain measurement technique*
- The reflected EM waves detected by a VNA for resolving amplitude and phase of each reflected signal
- **Goal:** accuracy $\pm 2^\circ\text{C}$ in a range of 350 – 1000°C and spatial resolution <10 cm



Joint-time-frequency domain interrogation of multi-point FPI in a single cable for distributed sensing with high spatial resolution

Technical Challenges

- Unavailability of MCCC
- Materials for the MCCC
 - *Conductors – stability and properties*
 - *Insulator and reflector – stability and properties*
- Understandings of parametric effects
 - *Dimensions of reflector*
 - *Inter-reflector length, d*
 - *Insulator and reflector ϵ_r*
 - *Operating frequency range ...*

Proposed Research, Tasks, and Status

Task/ Sub-task#	Project milestone description	Project Duration – Start: 07/01/2014; End: 06/30/2017												Planned end date & status
		Project Year 1 (7/1/14-6/30/15)				Project Year 2 (7/1/15-6/30/16)				Project Year 3 (7/1/16-6/30/17)				
		Q1	Q2	Q3	Q4	Q5	Q6	Q7	Q8	Q9	Q10	Q11	Q12	
1.0	1. Management Plan and team building	•												7/31/14
2.1	1. Design the MCCC-FPI sensor.	•	•											Completed 12/31/14
2.2	2. Identified materials for MCCC-FPI to withstand up to 1000°C in relevant gases		•	•	•									6/30/15
3.1	1. Fabricated the single-point MCCC-FPI sensor and demonstrated single-point measurement up to 500°C with accuracy of ±2°C (GO/NO-GO)				•	•	•							12/31/15
3.2	2. Designed multi-point MCCC-FPI sensor and established instrument and software for distributed sensing (Task 4.1)			•	•									Completed 6/30/15
4.1	1. Design cascaded MCCC-FPI sensors and develop instrumentation and algorithms for distributed sensing					•	•	•						Completed 12/31/16
4.2	2. Fabrication of the multiple-point MCCC-FPI sensor (2 -3 FPI)							•	•	•				12/31/16
5.0	1. Fabricated Multipoint FPIs (16 Pts) in ~2m-long MCCC. 2. Demonstrated 16 FPIs in ~2m-long MCCC for distributed temperature measurement up to 1000°C with spatial resolution <10cm.										•	•	•	6/30/17 On-Going 6/30/17

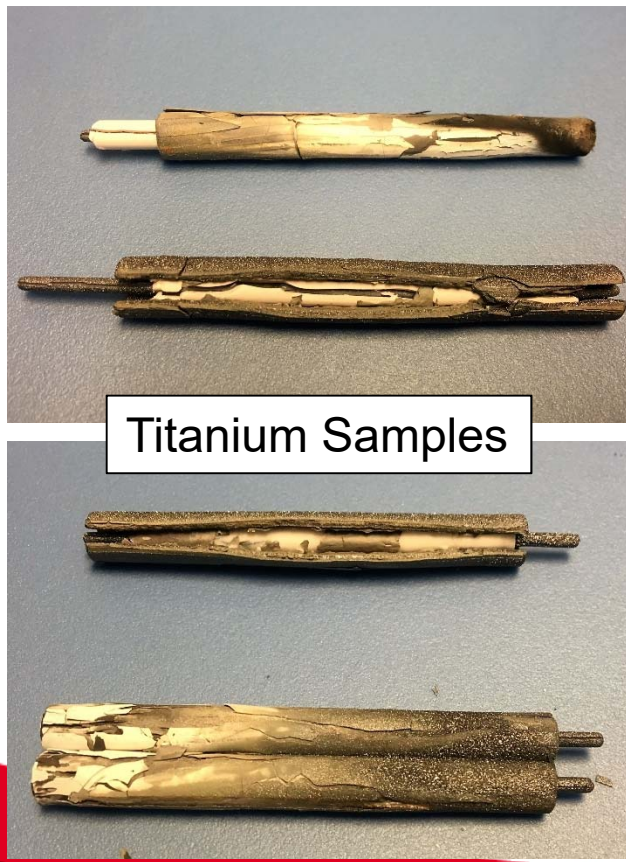
1. Materials selection and development for MCCC

Candidates of Materials for MCCC

<u>Conductor</u>	Composition	CTE (10^{-6} m/m °C)	Tm (°C)	Elec. Resistivity
S.S. (316L)	Fe w/ 16-18%Cr, 10-14%Ni, 2%Mo, 0.75%Si	19.9	1400	690 nΩ·m
Titanium	>99.2% Ti	8.55	1670	420 nΩ·m
<u>Dielectric Material</u>	Composition	CTE (10^{-6} m/m °C)	Max Op. Temp (°C)	Dielectric Constant @ 1 MHz
Al ₂ O ₃	99.5% Al ₂ O ₃	8.1-8.4	1750	9.8
Mullite	59% Al ₂ O ₃ 36%SiO ₂ 3%K ₂ O	5.9	1500	5.8
ZTA	Zr-Al ₂ O ₃	8.1	1650	10.6
Sapphire	Al ₂ O ₃	5.4	2000	9.3 – 11.5
Macor [®]	SiO ₂ -ceramic	9.4	1000	6.03
Fused Quartz	SiO ₂	0.6	1000	3.8
Air	(N ₂ + O ₂)	Compressible	>2000	~1.0

MCCC Structural and Mechanical Stability

- Stainless steel (tube and wire) and dense α -alumina tubes have been selected as the basic materials for MCCC construction

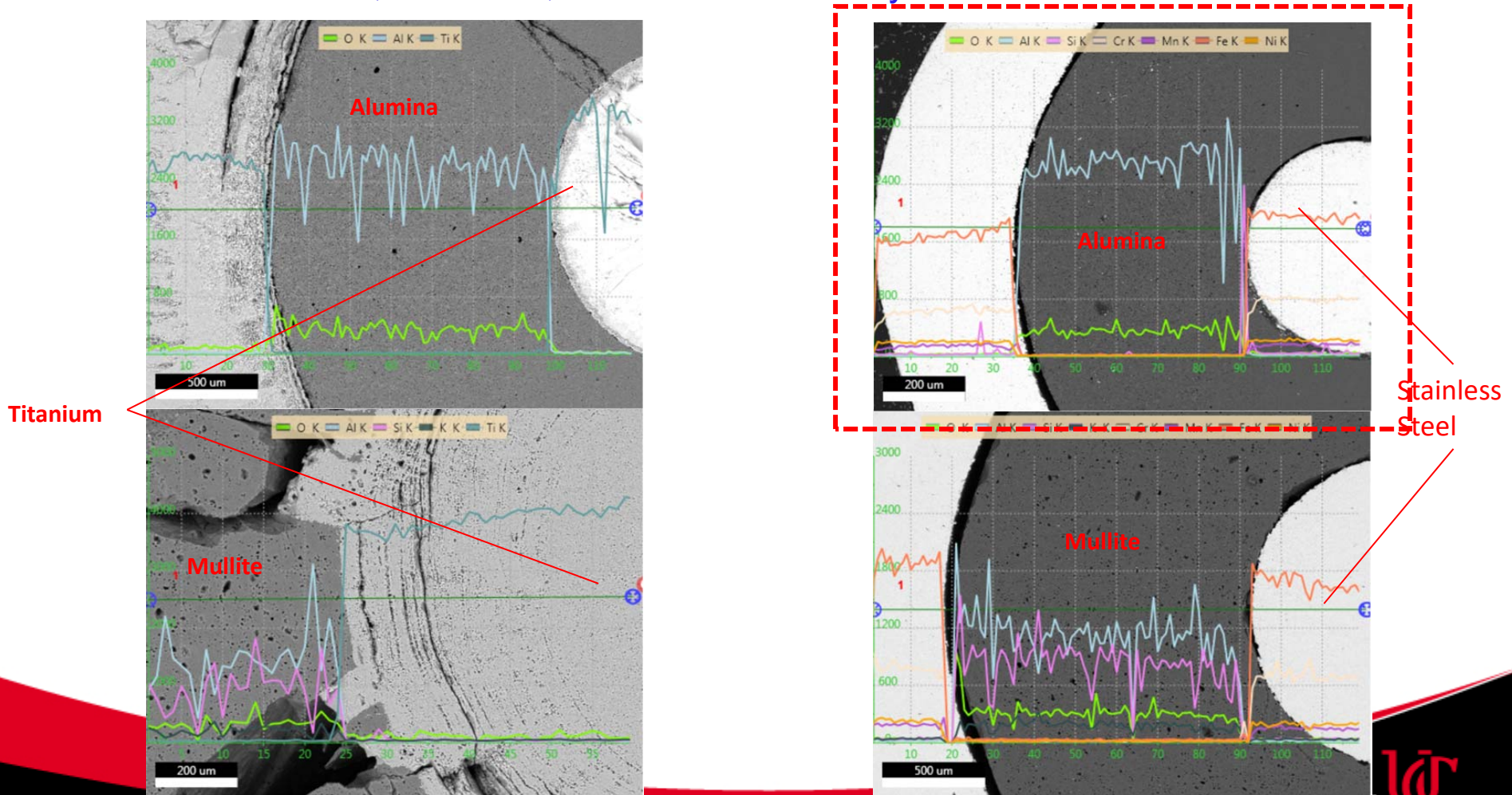


After 500 hours in direct contact with gas mixtures containing syngas and steam at 1000°C



MCCC Structural, Chemical, and Thermal Stability

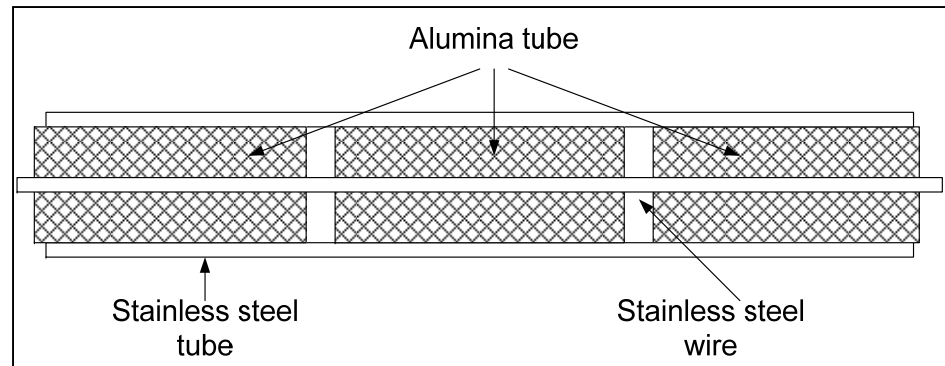
- Stainless steel (tube and wire) and α -alumina tubes combination exhibited the best structural, chemical, and thermal stability



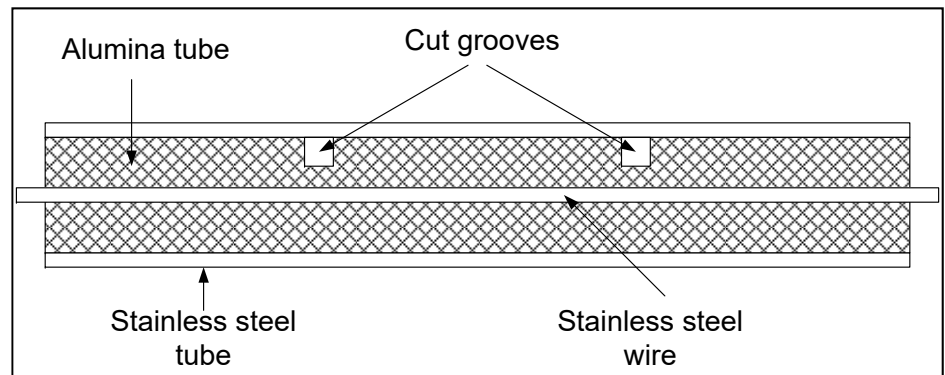
2. Fabrication and evaluation of single-point MCCC-FPI

MCCC-FPI Sensor Design

Type *a*: Gap/Whole disc reflector with ceramic insulation

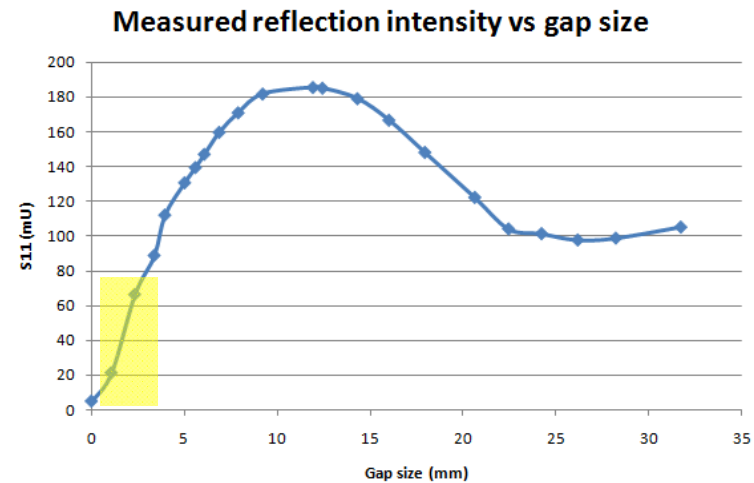
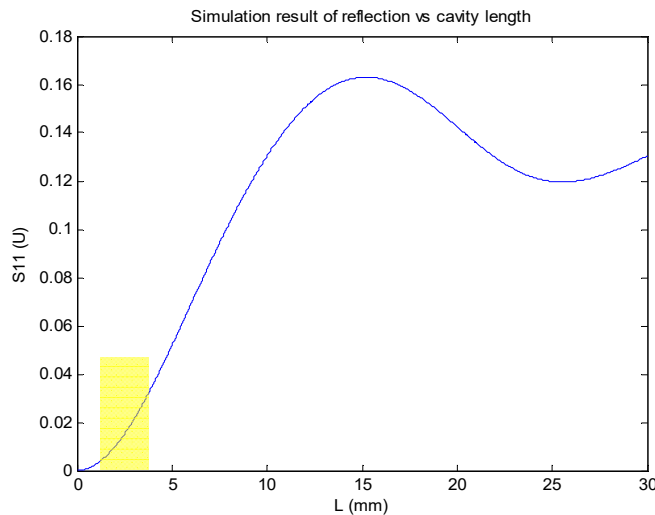
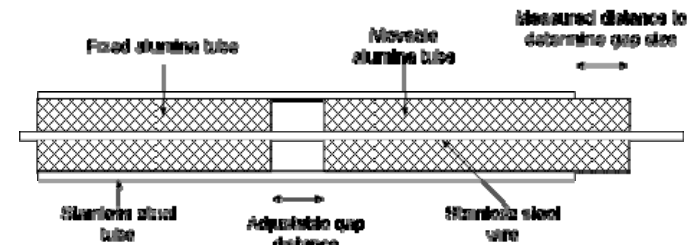


Type *b*: ceramic insulation with groove reflectors



MCCC-FPI: Gap Size Determination

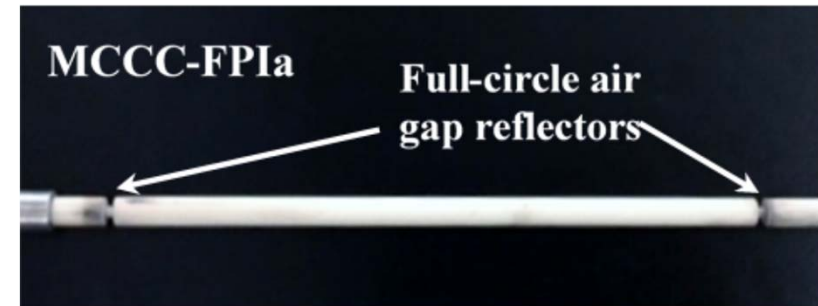
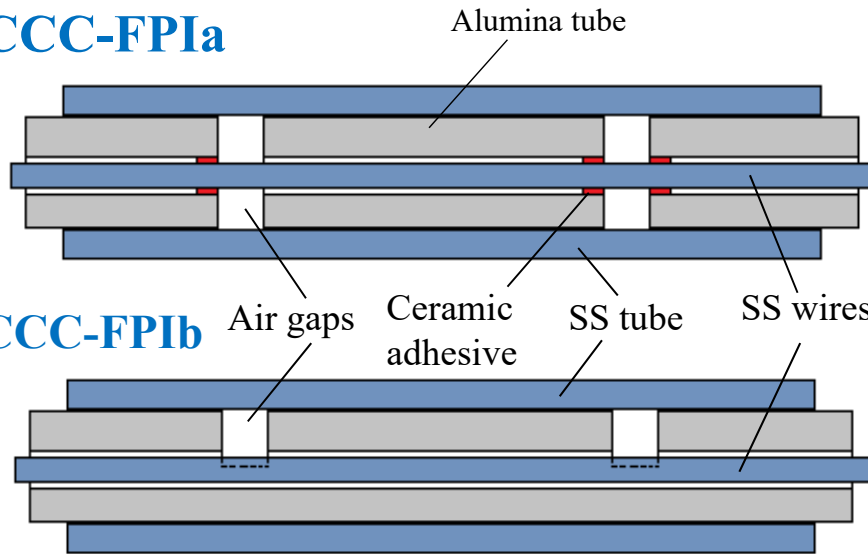
- A reflection of appropriate intensity is desired especially for development of single-cable multiplexed distributed sensors
- Air gap width of 1 – 4 mm appears to be suitable for sensor applications



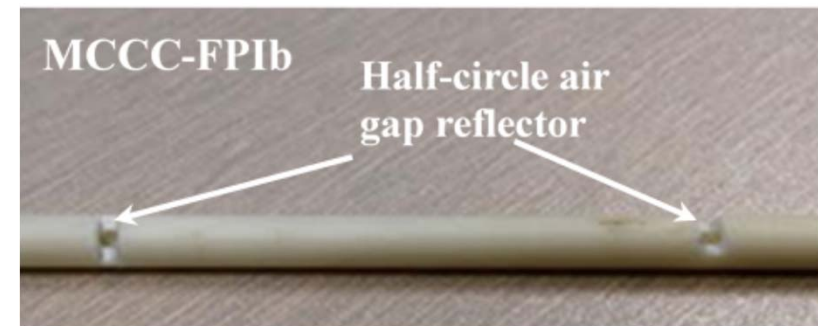
Model-predicted (left) and experimentally measured (right) reflection intensity as a function of reflectors' width.

Single-Point MCCC-FPI Structures

MCCC-FPIa

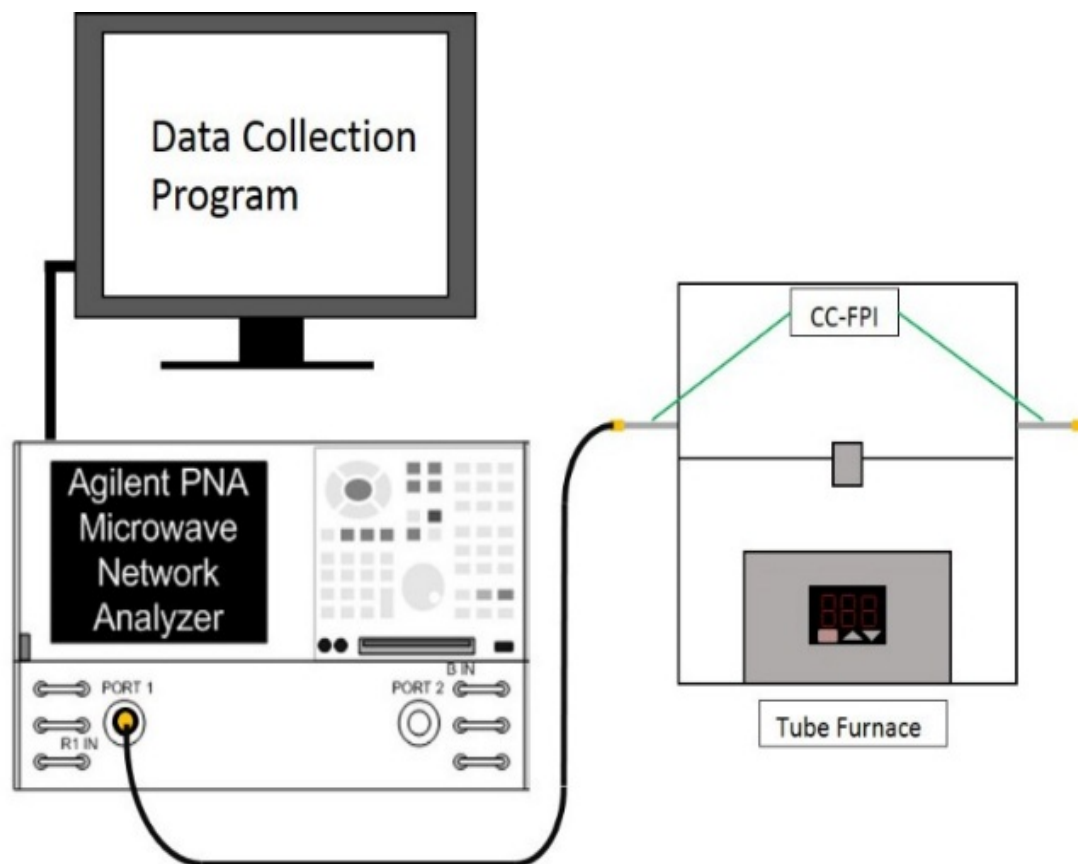


MCCC-FPIb

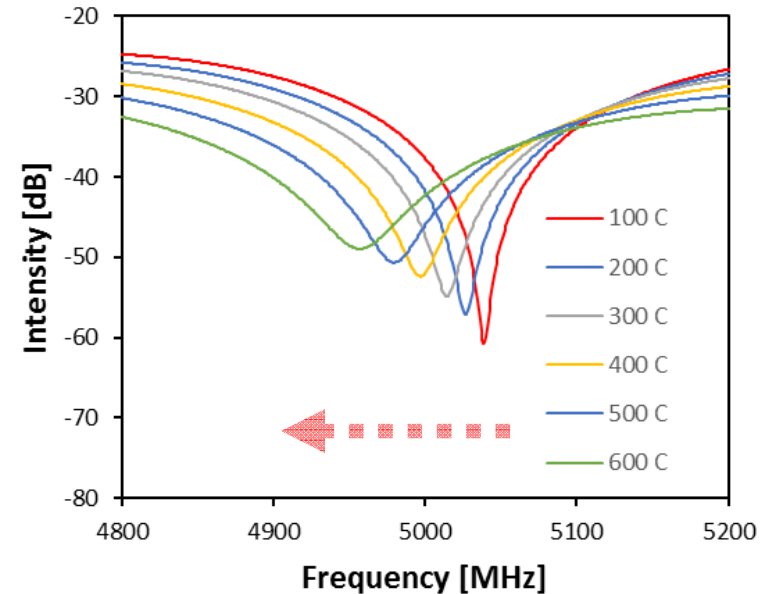
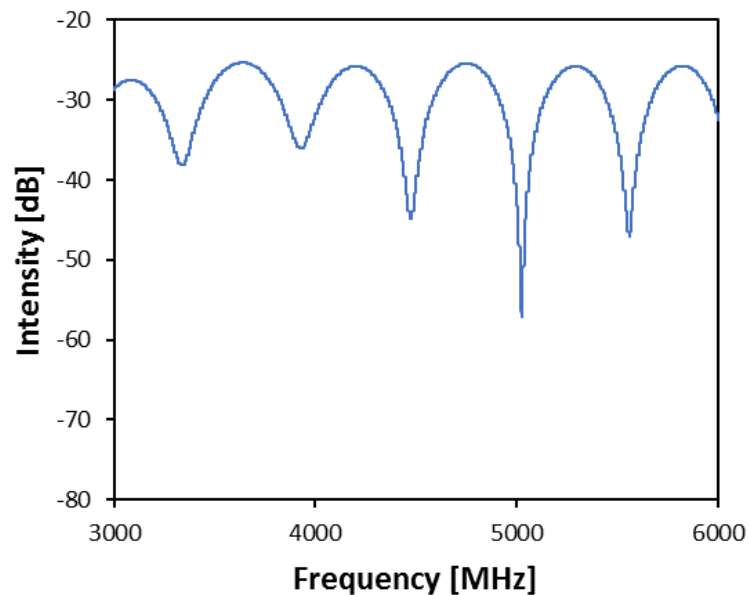


- **MCCC-FPIa**: d determined by expansion/contraction of metal wire
- **MCCC-FPIb**: d determined by expansion/contraction of Alumina tube

Sensor Operation Apparatus

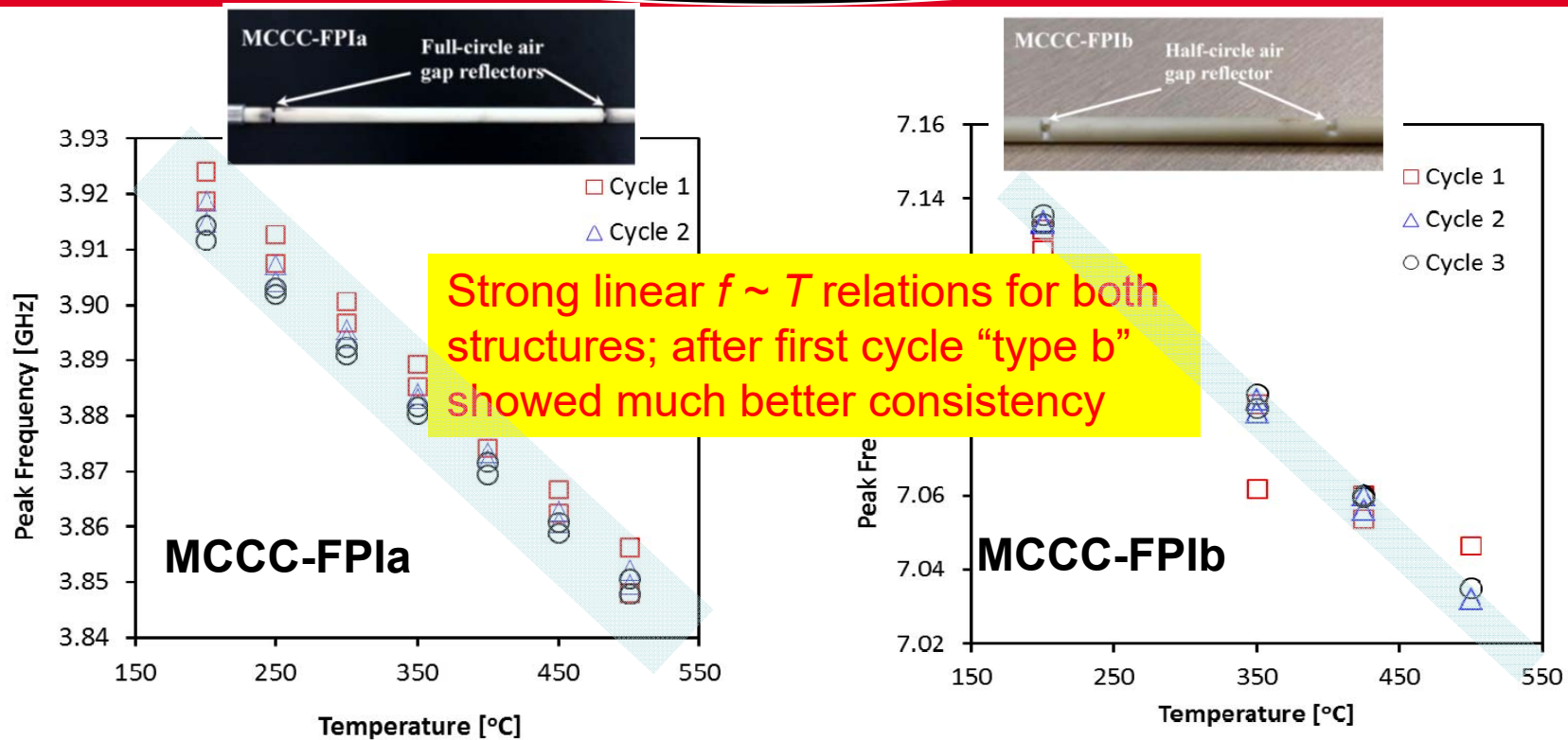


Interferogram Evaluation as a Function of Temperature



Shift of resonant frequency as temperature increases (MCCC-FPIa)

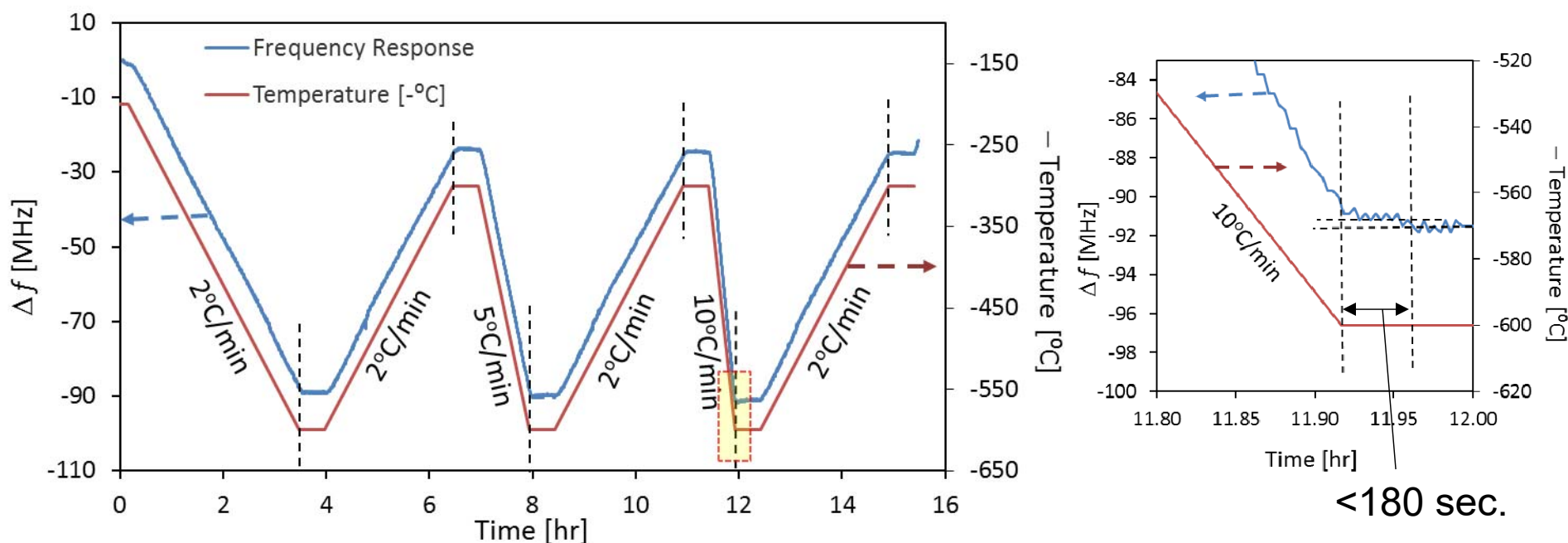
Correlation between Frequency and Temperature



Evolution of the relationship between resonant frequency and temperature during heating-cooling cycles

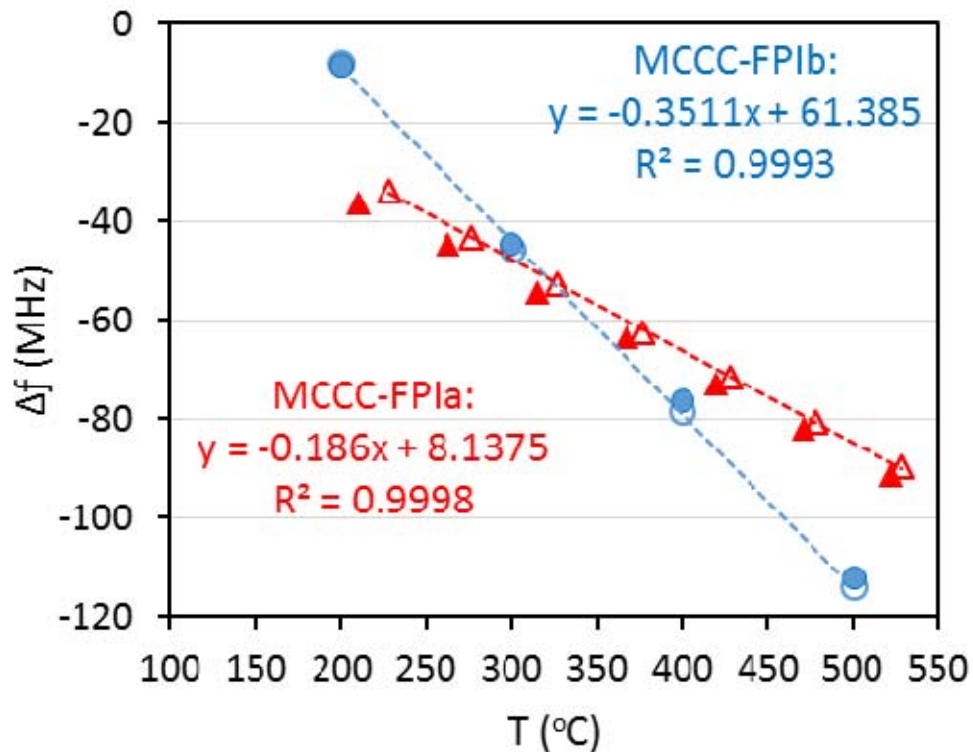
Sensor Response Speed

Frequency shift (Δf) for MCCC-FPIa as a function of time in response to the programmed temperature change



The response time is reasonably short and may be acceptable for the harsh environment measurements

Temperature-Dependence of Δf and Sensitivity



Resonant freq. used @ RT:

FPIa – 3.4 GHz; FPIb – 7.1 GHz

Temperature-dependences of Δf :

Excellent linear dependence –

FPIa (-0.186 MHz/°C)

FPIb (-0.351 MHz/°C)

Sensitivity:

FPIb higher than FPIa

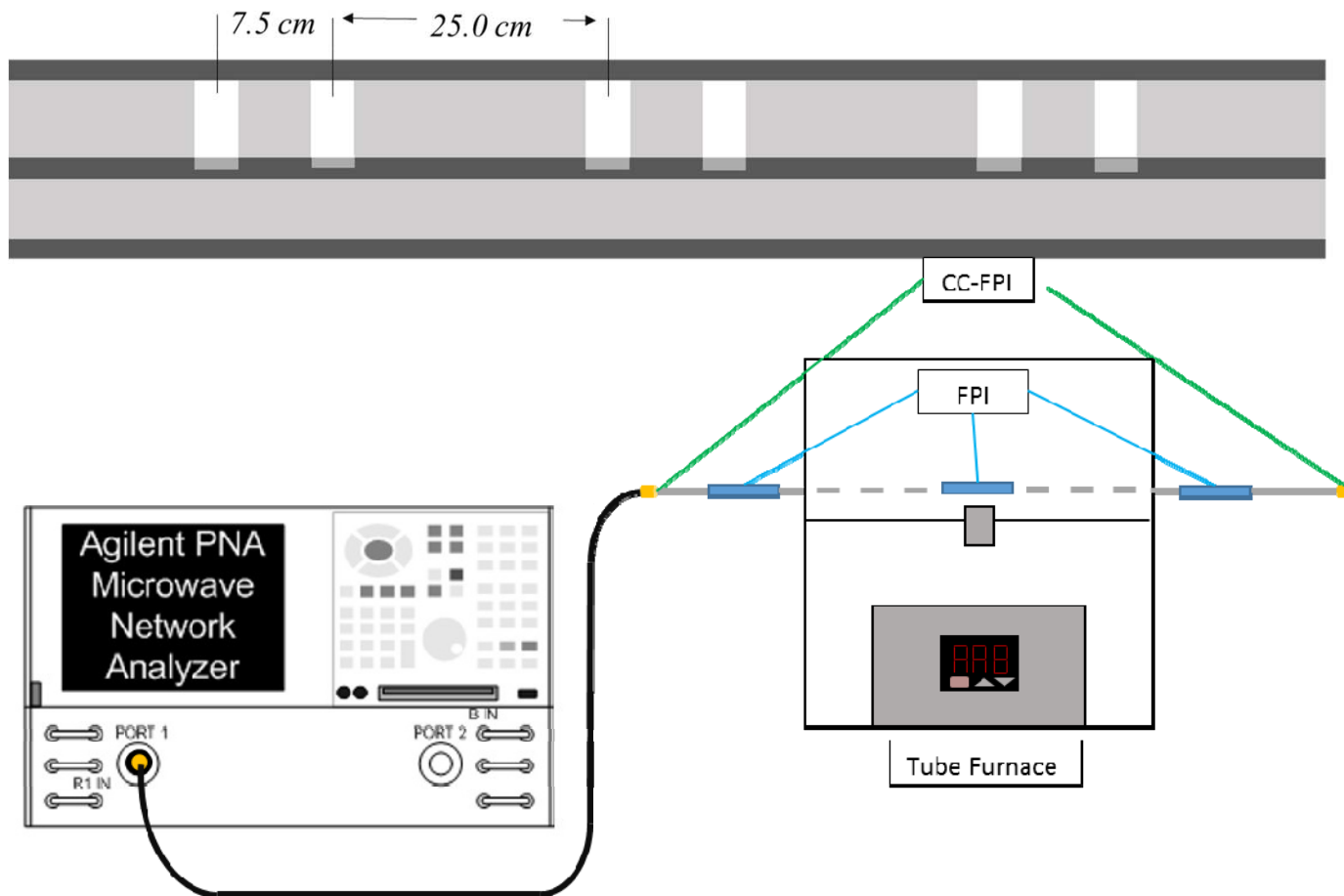
Structure stability:

FPIb better than FPIa

Experimentally measured frequency shift Δf as a function of temperature for both MCCC-FPI with linear correlations

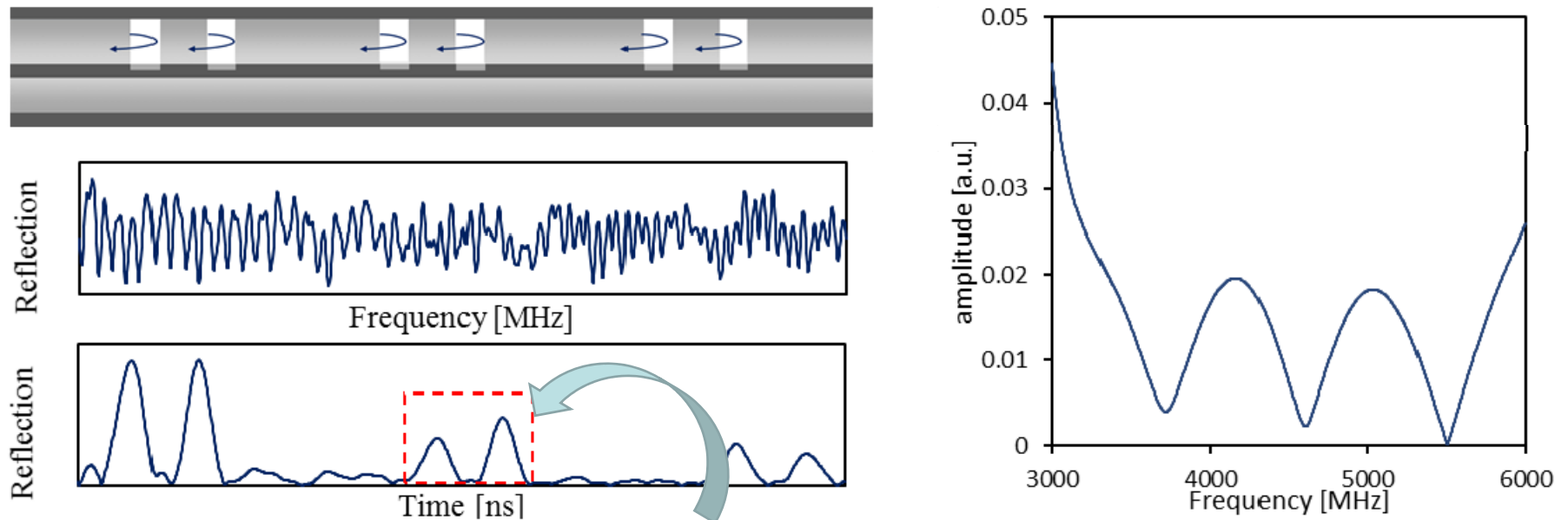
3. Design and fabrication of 2- or 3-point MCCC-FPI

3-Point MCCC-FPI



3-Point MCCC-FPI

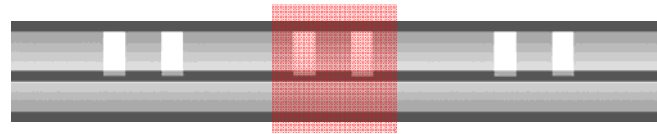
Joint-time-frequency domain operation.



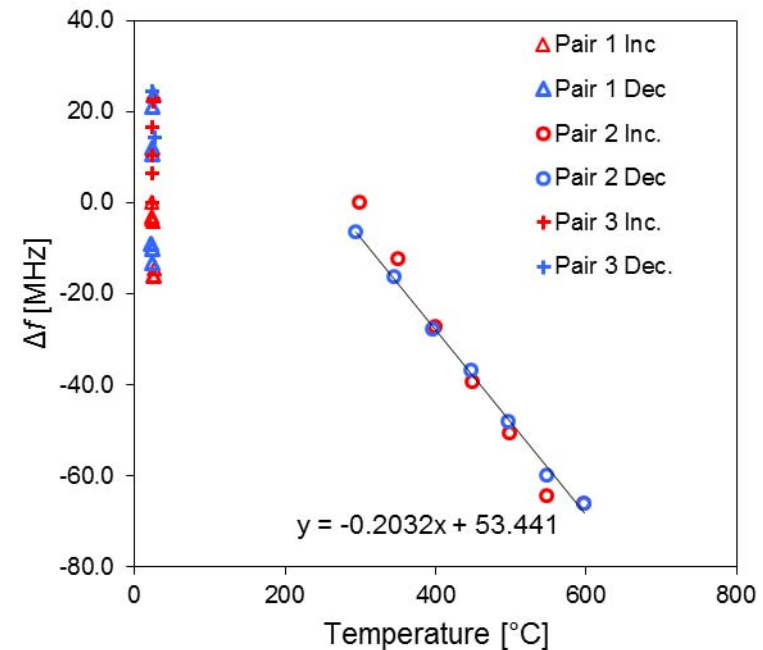
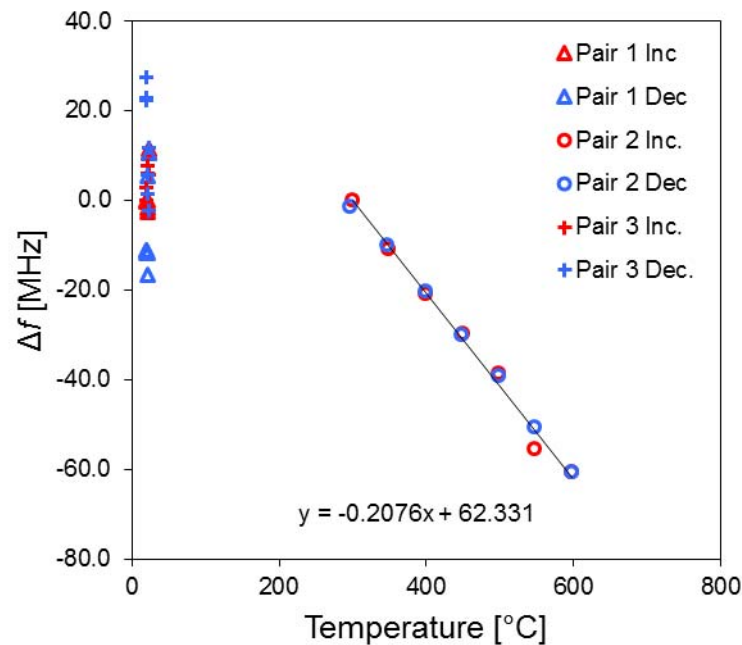
Red dashed box indicates gated FPI pair and its respective interferogram

3-Point MCCC-FPI

Cycle 1

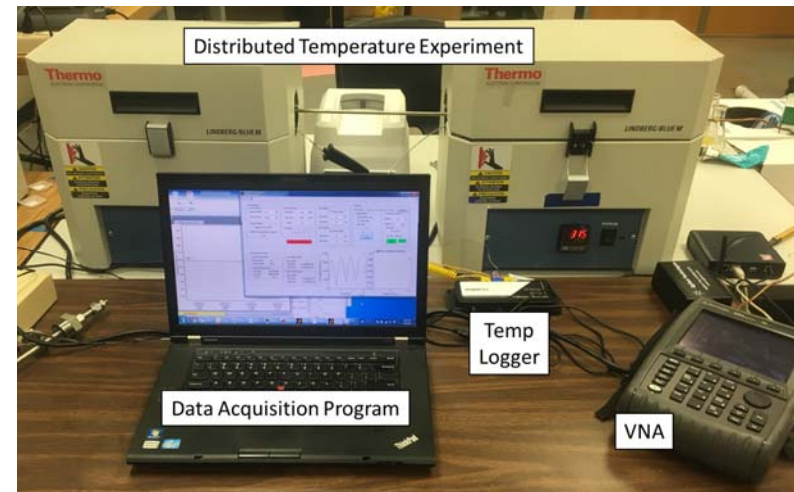
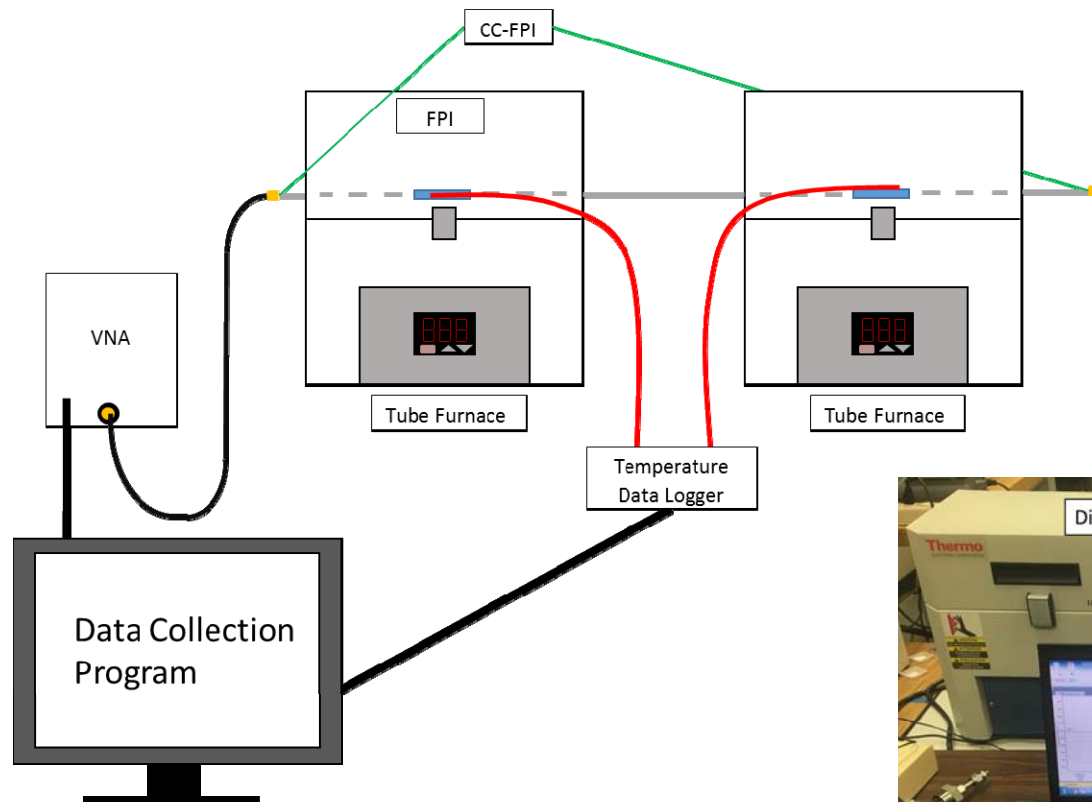


Cycle 2



Evolution of the relationship between resonant frequency and temperature during heating-cooling cycles. Pair 2 placed in center of tubular furnace.

Multi-Point MCCC-FPI

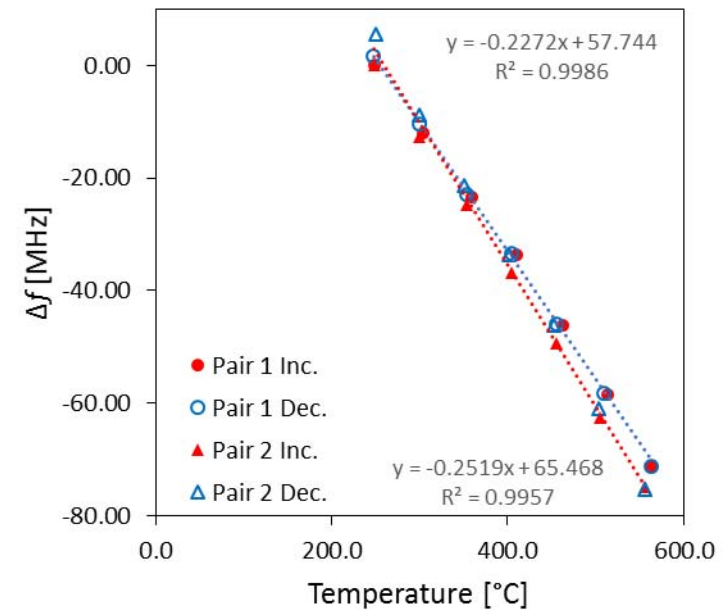
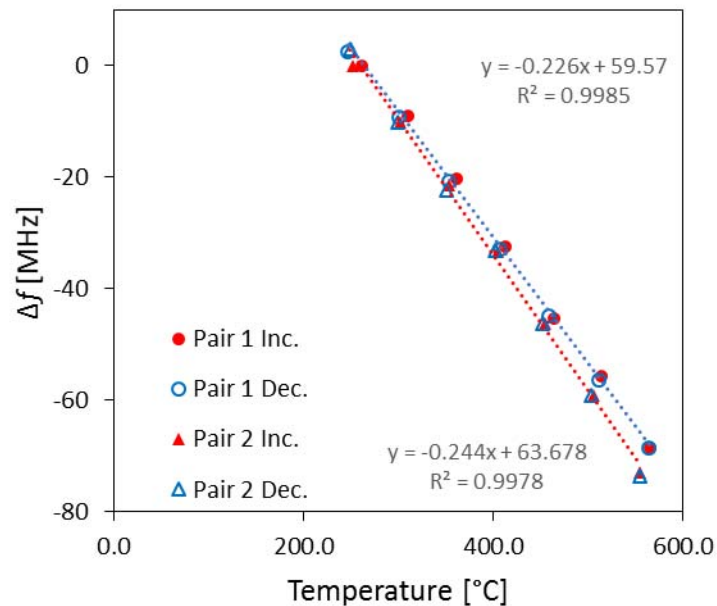


2-Point MCCC-FPI

Cycle 1



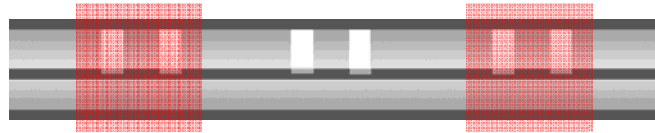
Cycle 2



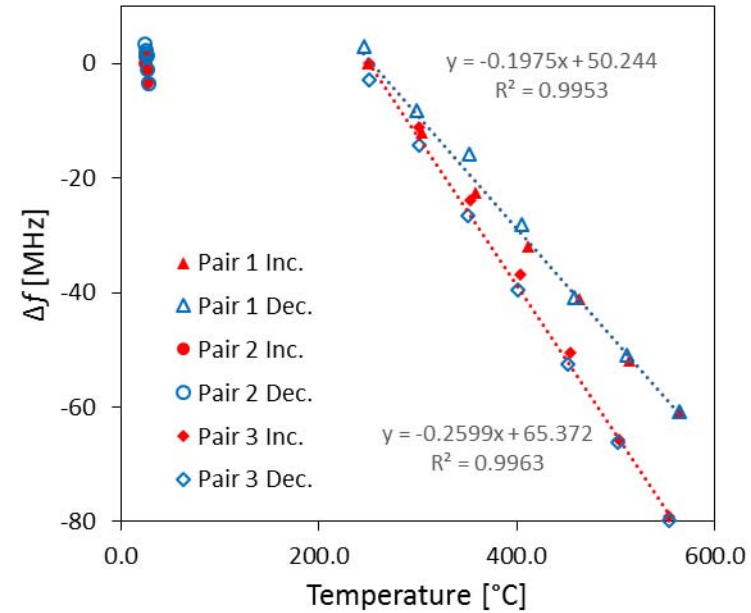
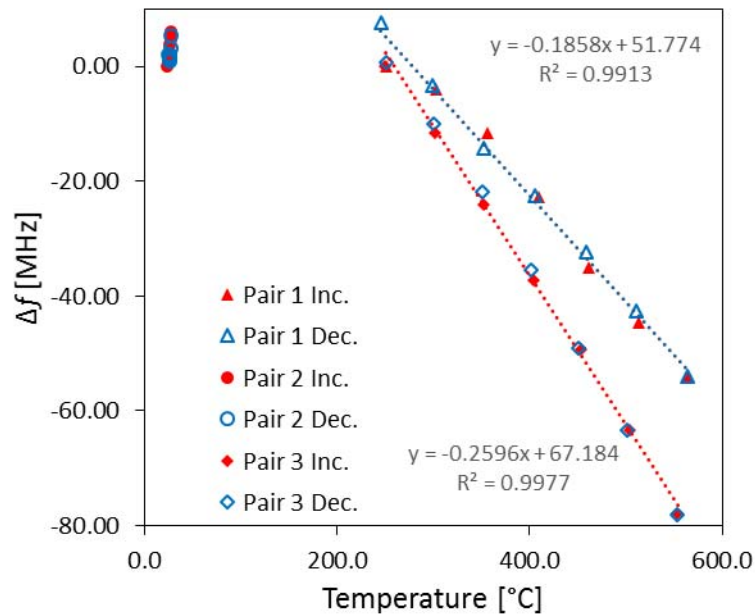
Evolution of the relationship between resonant frequency and temperature during heating-cooling cycles.

3-Point MCCC-FPI

Cycle 1

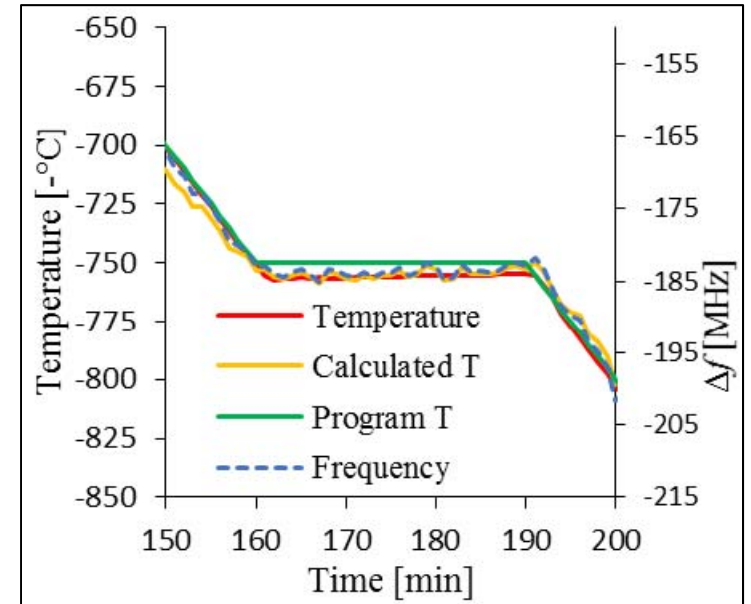
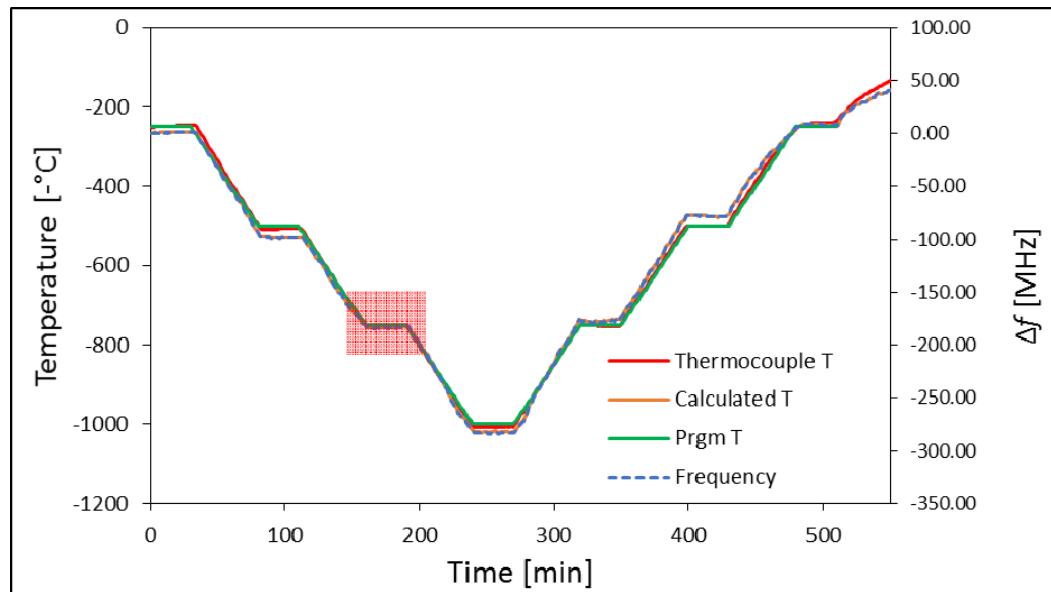


Cycle 2



Evolution of the relationship between resonant frequency and temperature during heating-cooling cycles.

Response of MCCC-FPI



Evolution of the relationship between resonant frequency and temperature during heating-cooling cycles.

4. Evaluation of multi-point MCCC-FPI (10-16
pts in ~2m-long MCCC)

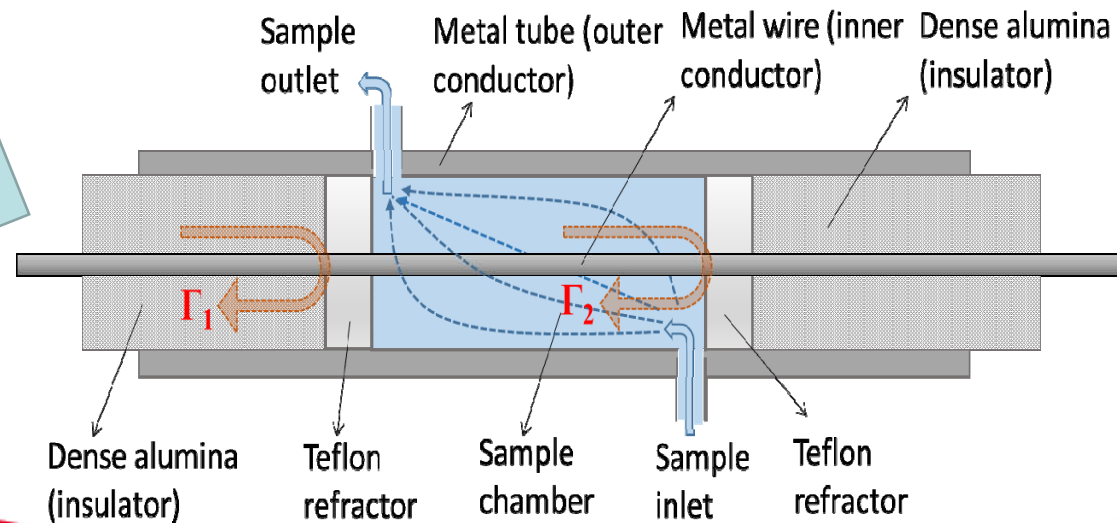
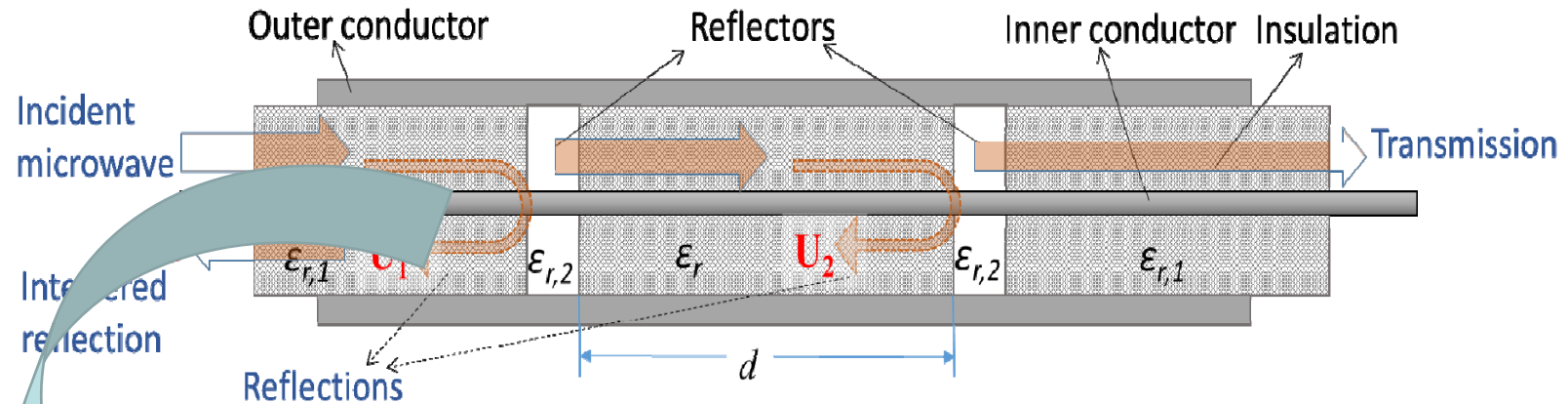
Research still ongoing

Summary

- Research progress of this project is on schedule
- Research accomplishments
 - Identified and developed metal ceramic materials for construction of MCCC-FPI sensors with good stability in harsh environments
 - Fabricated and demonstrate single point MCCC-FPI sensor for temperature measurement up to 1000°C
 - Fabricated and demonstrated MCCC-FPI sensor with 2 – 3 FPIs (2 – 3 sensing points)
 - Long cable (2m) multi-point (10pts) sensor under development

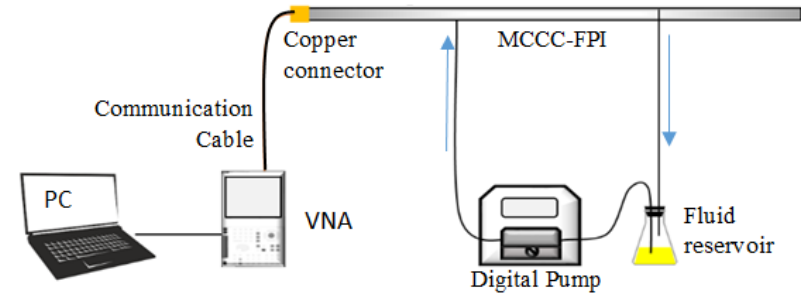
5. MCCC-FPI for dielectric constant measurements for sensor material development

Sensor Concept



Sensing Mechanism

$$f_N = \frac{Nc}{2d\sqrt{\epsilon_r}}$$

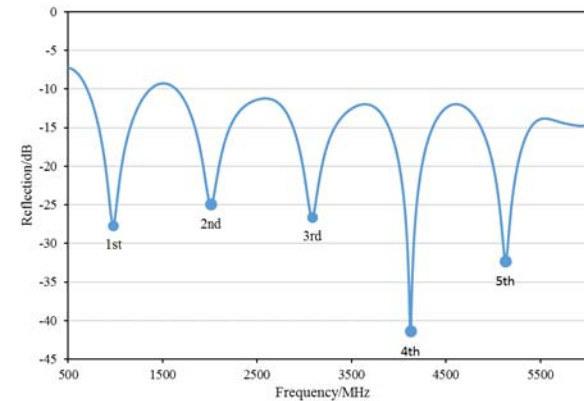


$$U_1 = \Gamma(f)e^{-\alpha z} e^{-j2\pi f \frac{2d_0\sqrt{\epsilon_{r,1}}}{c}}$$

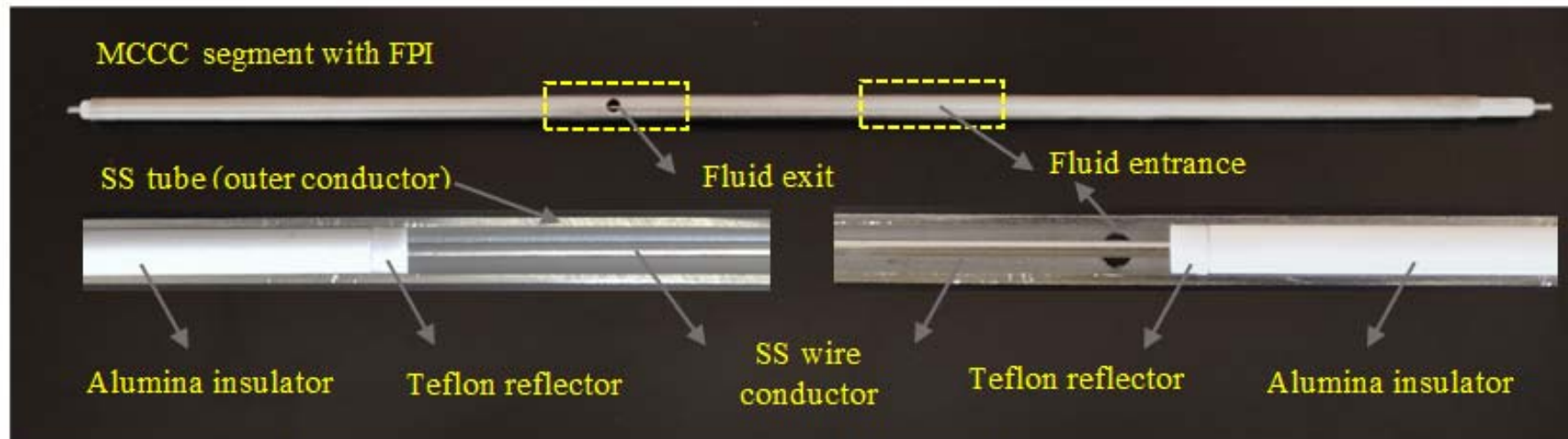
$$U_2 = -\Gamma(f)e^{-\alpha z} e^{-j2\pi f \frac{2d_0\sqrt{\epsilon_{r,1}} + 2d\sqrt{\epsilon_r}}{c}}$$

$$U = 2j \cdot \Gamma(f)e^{-\alpha z} e^{-j2\pi f \frac{2d_0\sqrt{\epsilon_{r,1}} + d\sqrt{\epsilon_r}}{c}} \sin\left(2\pi f \frac{d\sqrt{\epsilon_r}}{c}\right)$$

$$f_N = \frac{Nc}{2d\sqrt{\epsilon_r}}$$



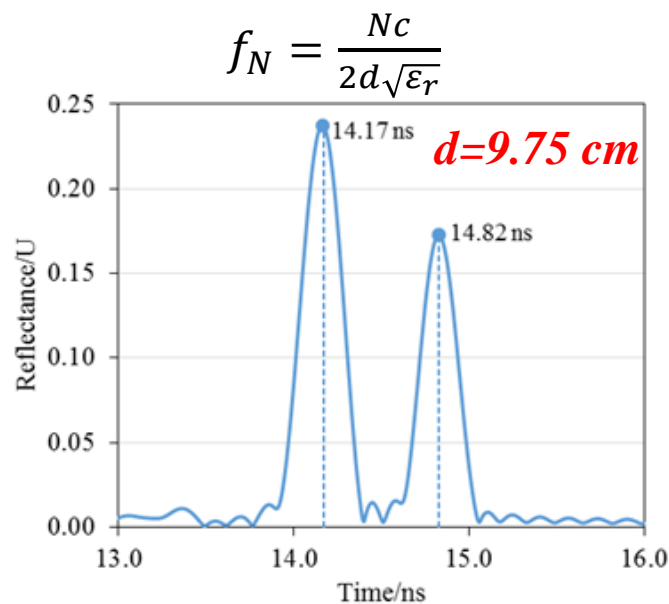
Sensor Construction



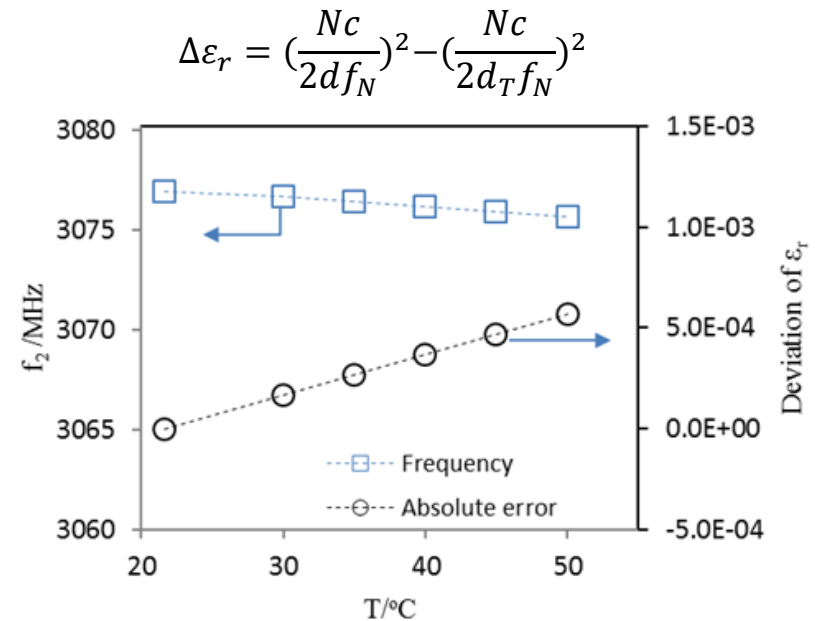
Photograph showing the structure of an actual MCCC-FPI microwave sensor and section

Determination of “d” Value

- The inter-reflector distance “d” is precisely determined from interferogram with dry air or vacuum ($\epsilon_r \sim 1.0$)
- Temperature effect on Δf at 20 – 50 C is negligible compared to effect of ϵ_r changes



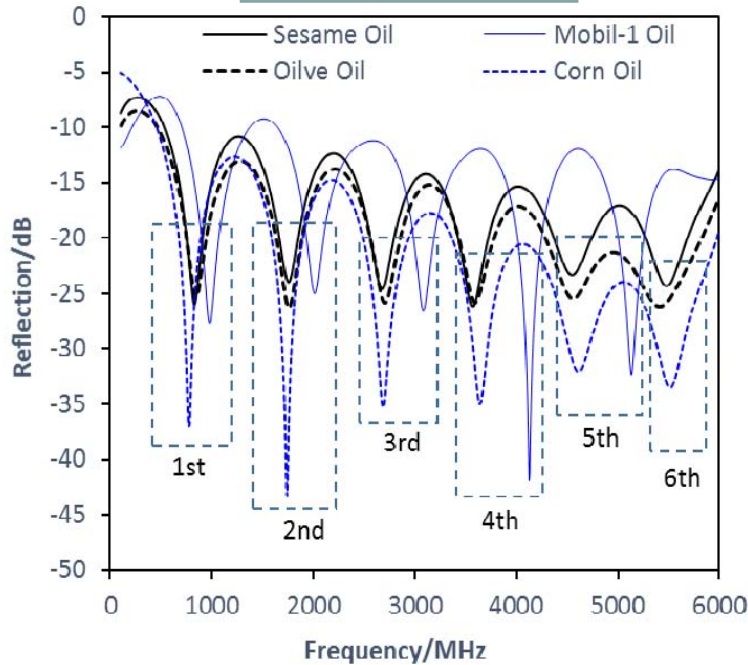
The time domain spectrum of the air-filled MCCC-FPI.



The 2nd resonant peak frequency (f_2) of dry air filled MCCC-FPI and the $\Delta\epsilon_r$ as functions of temperature.

Fluid Dielectric Constant Measurement

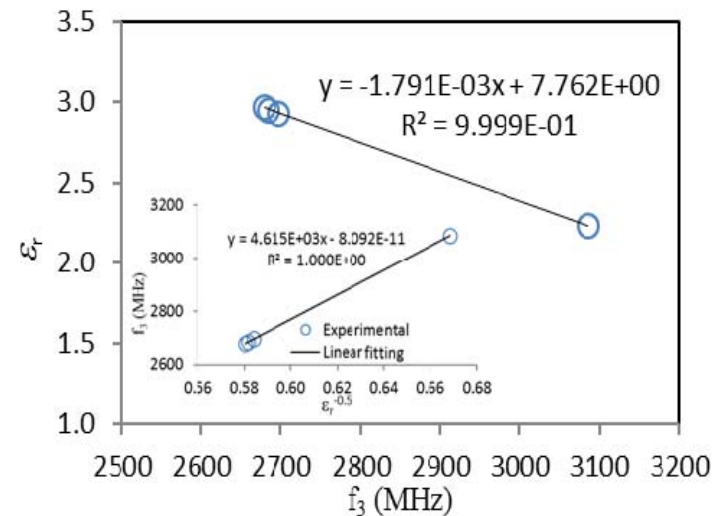
$$f_N = \frac{Nc}{2d\sqrt{\epsilon_r}}$$



The frequency domain interferometric reflection spectra of the MCCC-FPI when filled with sesame oil, olive oil, corn oil, and Mobil-1 oil, respectively.

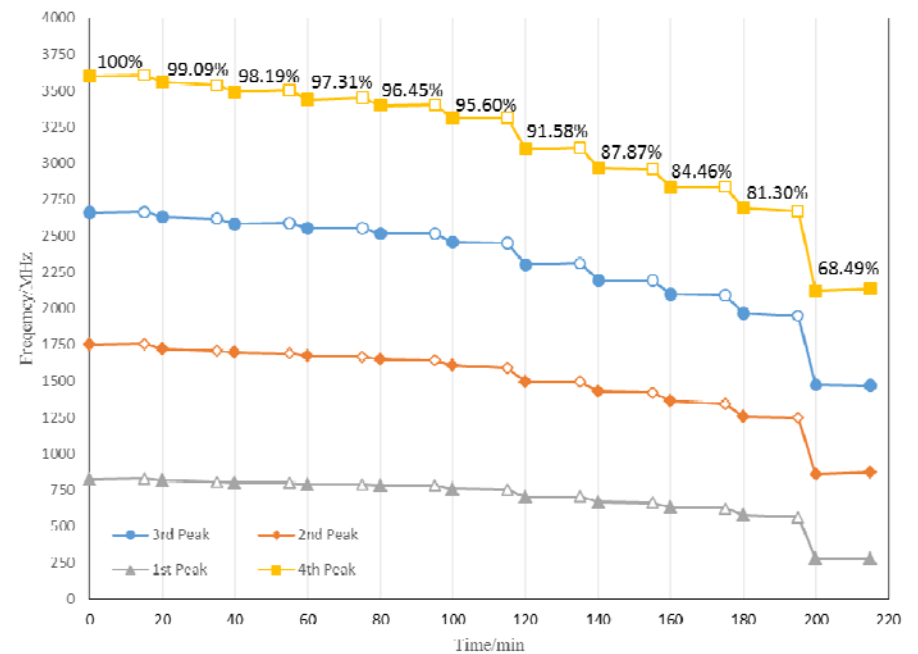
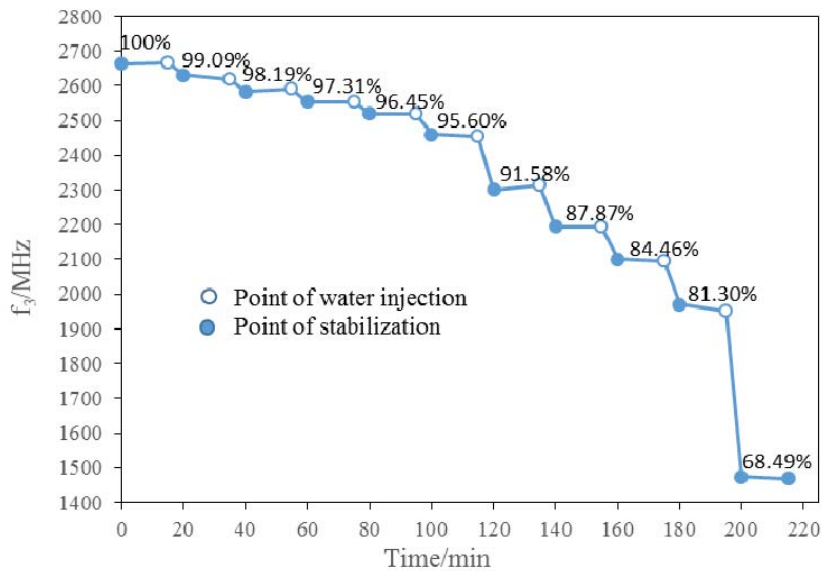
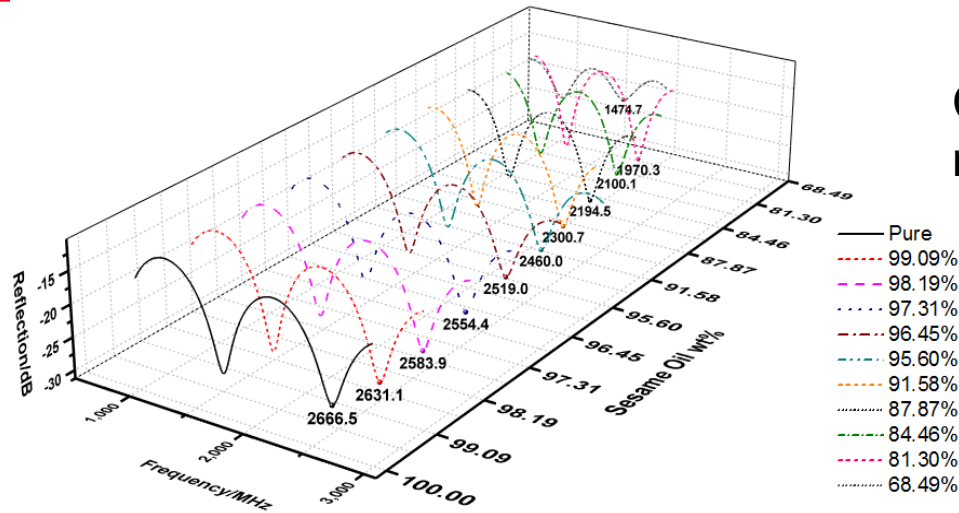
Dielectric constants of the oils measured at room temperature (24°C) by the MCCC-FPI in comparison with literature values

Oil	This work								Reference [11-16]	
	f_2 /GHz	ϵ_r	f_3 /GHz	ϵ_r	f_4 /GHz	ϵ_r	f_5 /GHz	ϵ_r	f /GHz	ϵ_r
Sesame	1.75	3.09	2.68	2.97	3.57	2.97	4.55	2.86	0.001~9	3.11~2.42
Olive	1.75	3.09	2.70	2.93	3.59	2.94	4.56	2.87	0.31~0.91	3.11~2.46
Corn	1.74	3.12	2.68	2.96	3.65	2.85	4.61	2.78	2.8~3.0	2.66~2.61
Mobil-1	2.02	2.33	3.08	2.24	4.12	2.23	NA	NA	NA	2.1~2.8



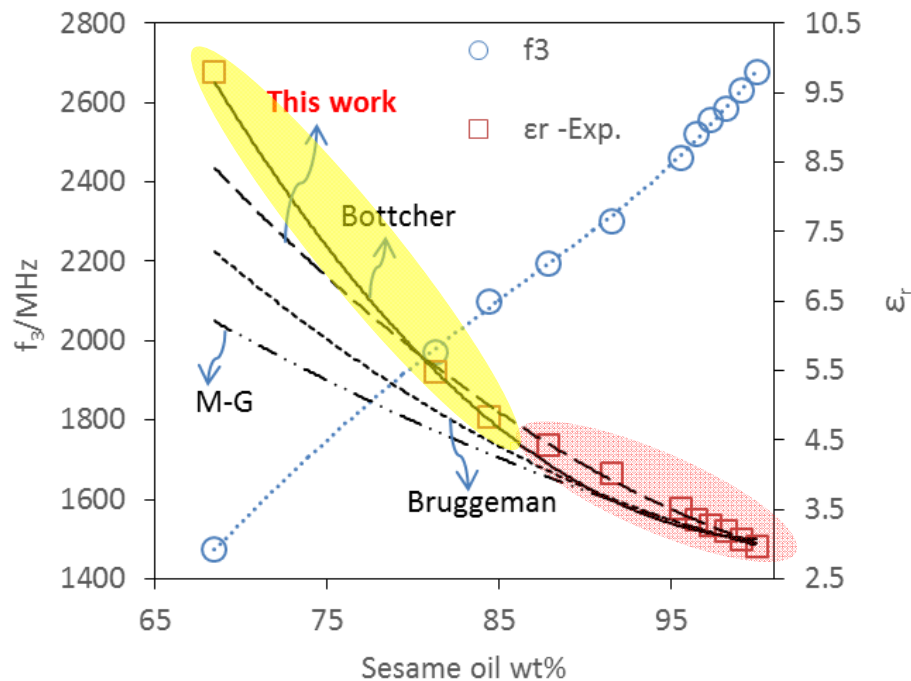
Online Monitoring of Fluid Dielectric Constant

Continuous monitoring of sesame oil/water mixture with varying water contents



Mixing Rule for ϵ_r of Mixtures

Comparison between experimental values and model predictions of $\epsilon_{r,mix}$ for sesame-water binary mixture



Maxwell-Garnett:
$$\frac{\epsilon_{r,mix} - \epsilon_{r,s}}{\epsilon_{r,mix} + 2\epsilon_{r,s}} = \frac{\epsilon_{r,d} - \epsilon_{r,s}}{\epsilon_{r,d} + 2\epsilon_{r,s}} \varphi_d$$

Bruggeman:
$$\frac{\epsilon_{r,mix} - \epsilon_{r,d}}{\epsilon_{r,s} - \epsilon_{r,d}} \left(\frac{\epsilon_{r,s}}{\epsilon_{r,mix}} \right)^{1/3} = 1 - \varphi_d$$

Bottcher:
$$\frac{\epsilon_{r,mix} - \epsilon_{r,s}}{3\epsilon_{r,mix}} = \frac{\epsilon_{r,d} - \epsilon_{r,s}}{\epsilon_{r,d} + 2\epsilon_{r,mix}} \varphi_d$$

Proposed mixing rule based on thermodynamic theory

$$\ln \epsilon_{r,mix} = \sum_i x_i \ln \epsilon_{r,i}$$

- The new mixing rule dramatically improved prediction at relatively low water content;
- The Bottcher's model performs well for high water content.

Conclusions

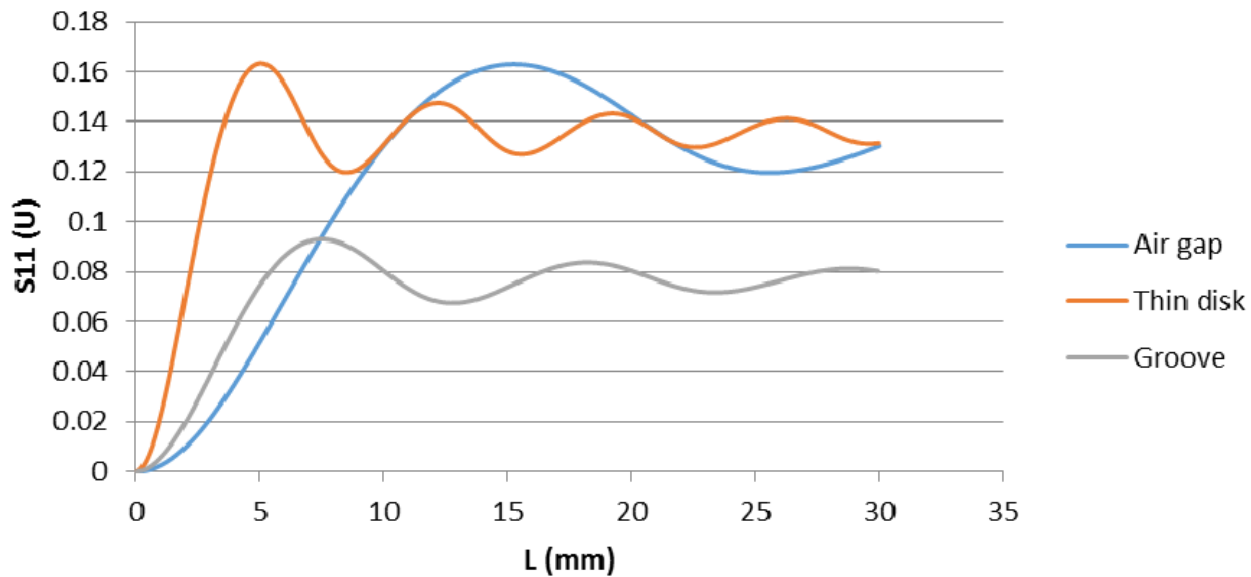
- Developed the MCCC-FPI sensor and establish its operating protocol and data processing models for measuring fluid dielectric constant in microwave frequency range;
- Developed new theoretical mixing rule for improved correlation and prediction of fluid mixture dielectric constant based on the knowledge of pure fluid dielectric properties; and
- The application of this sensor for measuring ϵ_r for packed ceramic powders is to be tested.

Q&A

Thank You

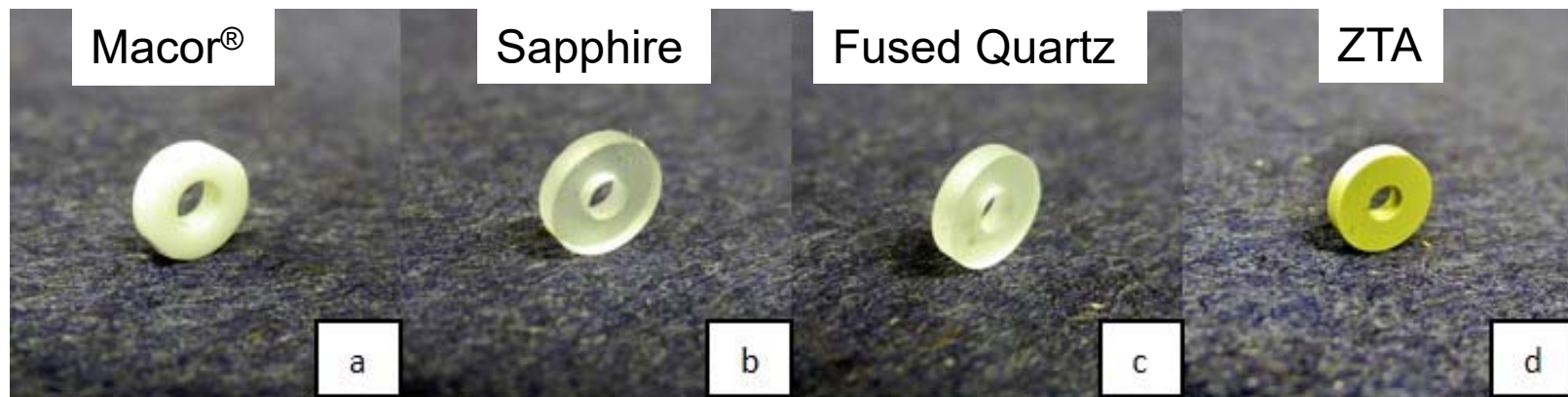
MCCC-FPI: Reflector width as a function of intensity

Simulation result of reflection vs cavity length of three structures

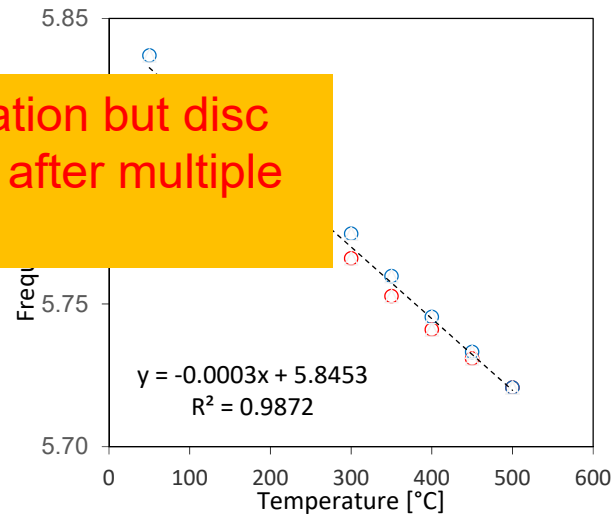
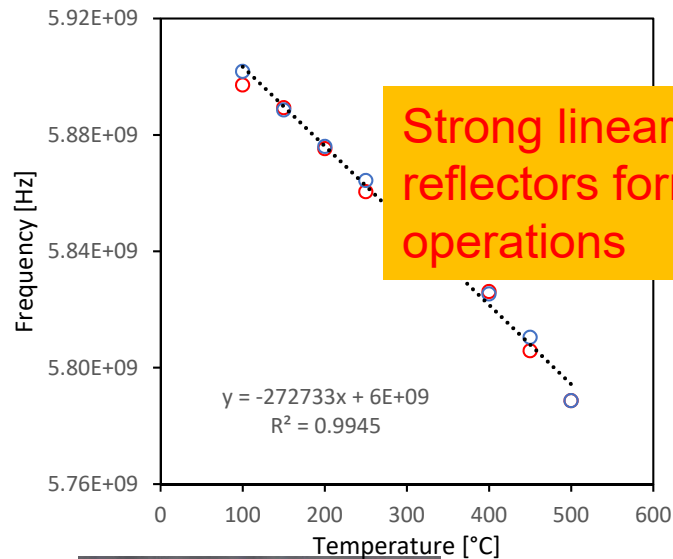


*Courtesy of Clemson

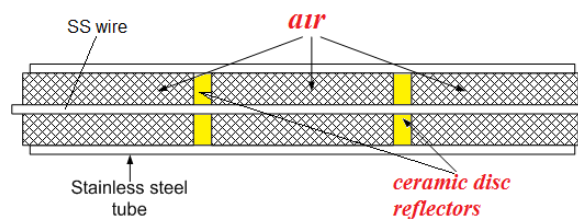
MCCC-FPI Materials: Reflectors



Single-Point MCCC FPI - Ceramic Disc-Alumina Dielectric

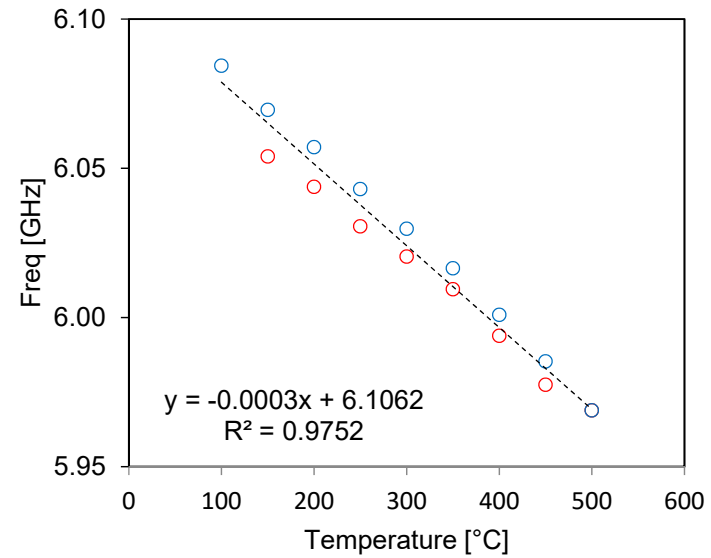
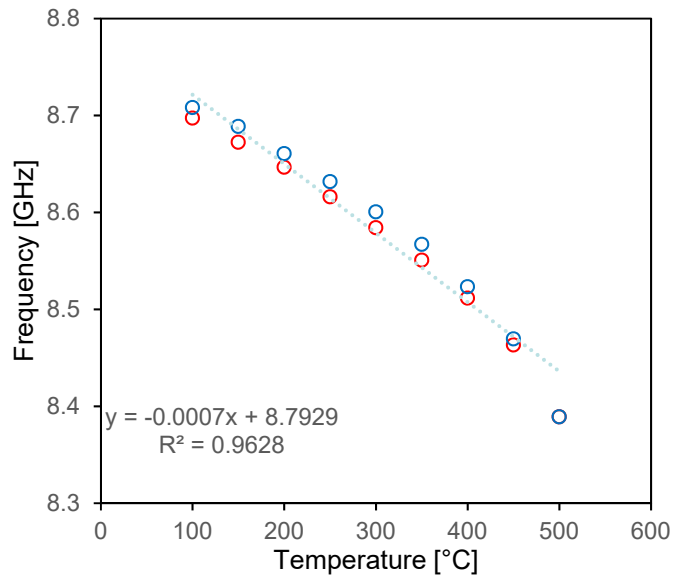


Strong linear $f \sim T$ relation but disc reflectors form cracks after multiple operations



Shift of resonant frequency as temperature increases

Single-Point MCCC FPI -Ceramic Disc-Alumina Dielectric



Shift of resonant frequency as
temperature increases

